*Acta Polytechnica CTU Proceedings* **37**:10–15, 2022
https://doi.org/10.14311/APP.2022.37.0010

Published by the Czech Technical University in Prague

# THE CHARACTERIZATION OF THE COLLIMATED BEAMS OF FAST NEUTRONS WITH THE CLID DETECTION SYSTEM

Martin Ansorge[a,b,*], Jan Novák[b], Mitja Majerle[b], Ján Kozic[a,b]

[a] *Czech Technical University in Prague, Faculty of Nuclear Sciences and Physical Engineering, V Holešovičkách 747/2, 180 00 Prague 8, Czech Republic*

[b] *Nuclear Physics Institute of the Czech Academy of Sciences, 250 68 Řež, Czech Republic*

[*] corresponding author: ansorge@ujf.cas.cz

Abstract. A new detection device for the measurements of light ions (p, d, t, $\alpha$) emitted as the products of the nuclear reactions induced by fast neutrons (5-33 MeV) was recently developed at the Nuclear Physics Institute of the Czech Academy of Sciences. The main objective of the Chamber-for-Light-Ion-Detection (CLID) is to produce new differential nuclear data of high interest for the material applications related to fusion and aerospace technologies and to potentially test and validate models of nuclear reactions. Hereby the experimental set-up for the measurements with the CLID is described in detail. The experimental characterization of the collimated fast neutron beams produced by the cyclotron-driven converter (p(35 MeV)+Be(2.5 mm)) is presented. In particular, the implementation of the Proton-Recoil-Telescope technique used for neutron energy spectra determination with the CLID is described.

Keywords: NPI, collimated fast neutron beams, cyclotron U-120M, CLID, Proton-Recoil-Telescope.

## 1. Introduction

A new 1.6 m long collimator coupled to a new neutron converter (based on the p+$^{9}$Be reaction) driven by the isochronous cyclotron U-120M was constructed at the Nuclear Physics Institute of the Czech Academy of Sciences (NPI-CAS). Collimated beams of fast neutrons are bringing new experimental possibilities, especially for on-beam measurements with semiconductor detectors which need to be shielded from intense neutron fields. The new vacuum chamber with the telescopes composed of silicon detectors allows us to perform precise measurements of double-differential cross sections of (n,cp - charged particle) reactions induced by fast neutrons with kinetic energies from 5 to 33 MeV. Motivated by the development of future fission and fusion energy projects, the nuclear data measurements of cross sections for nuclear reactions induced by fast neutrons are of high interest.

In recent years, the CLID detection system was commissioned and it delivered its first experimental data. This paper describes the characterization of the collimated neutron fields available at the U-120M facility at the NPI-CAS. The neutron fluxes and energetic spectra were measured in the irradiation position of the CLID device using the experimental set-ups with the vacuum chamber as well as with the scintillation probes.

The development of the CLID system follows the previous development of similar devices used at several nuclear research facilities worldwide. During past decades, the DDCS data for (n,cp) reactions induced by fast neutrons (10-200 MeV) on several basic elements (C, Li, O, Al, Si, Fe, Co, Bi, U, etc.) were measured and published at LANSCE in USA [1], at CYCLON in Belgium [2–4], at Crocker nuclear laboratory in the USA [5–7] or at Svedberg laboratory in Sweden where the Medley chamber was constructed and used for several campaigns of DDCS measurements [8–11]. Recently, the Medley was moved for the new set of experimental campaigns to the GANIL laboratory in France where the new LINAC accelerator is used for neutron production mainly in the energy region from 1 to 40 MeV [12]. In 2022, new data on $\alpha$-particle production double differential cross-sections on carbon were published by the Chinese group from the CSNS facility for the energy range from 6 to 102 MeV [13].

## 2. General set-up for CLID experiments

The initial proton bunches are accelerated by the cyclotron U-120M to the kinetic energy of 34.8±0.5 MeV. Pulsed beams of primary protons are delivered through few meters of ion beam-line to a thin beryllium-based neutron converter where fast neutrons are produced. The neutron converter is placed very close to the 1.6 m long circular-shaped collimator (3 cm in diameter). Behind the collimator, the evacuated reaction chamber is placed at an approximate distance of 2.5 m (from the neutron converter to the irradiated sample). The representative schematics of the experimental set-up is shown in Figure 1.

### 2.1. Cyclotron-driven Neutron Source

The new neutron converter consists of 2.5 mm thick beryllium slab. The neutrons with quasi-

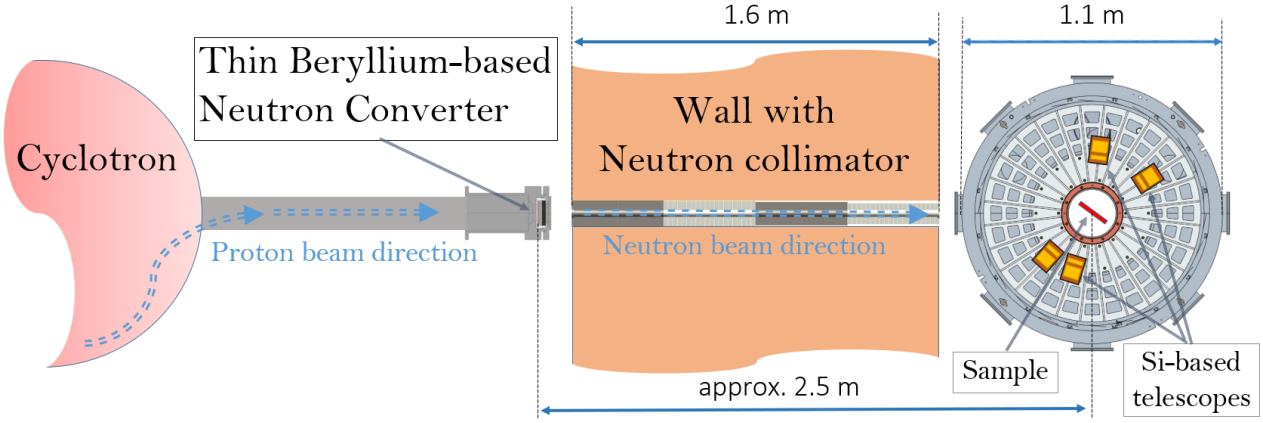


FIGURE 1. The top-view schematics of the experimental set-up used with the reaction chamber.

monoenergetic (QM) spectrum are produced by $^{9}$Be(p,n) reactions. The beryllium is backed by 10 mm thick slab of graphite which is used to stop the protons. The beryllium/graphite slabs are cooled by the flow of de-mineralized water. The primary proton beam current is measured by the integration of the charge deposited by protons in the beryllium/graphite slabs.

Historically, the QM neutron spectra produced by beryllium targets were already studied at the NPI-CAS. A 0.5 mm thick beryllium target was bombarded by ≈30 MeV protons and the neutron energy spectra were measured by the Time-of-Flight (ToF) technique using the NE-213 scintillator [14]. Two monoenergetic peaks separated by 2-3 MeV were recorded on the neutron continuum. Based on these results, five times thicker beryllium slab was chosen to produce only one broader peak of monoenergetic neutrons on continuous neutron background.

The target station with the neutron converter is placed close to the collimator wall as shown in Figure 1. A hollow steel cylinder was implemented in this wall. To shape the beam of fast neutrons, several hollow cylinders made of polyethylene and steel pieces were inserted in the inner part of the collimator cylinder. The rest of the collimator wall consists of the mixture of iron and water.

## 2.2. CLID DEVICE

Inspired by the Medley setup [8], a new vacuum chamber for the detection of light ions (p, d, t, $^{3}$He, $\alpha$) produced in nuclear reactions induced by fast neutrons (up to 33 MeV) was constructed at the NPI-CAS. The chamber allows the measurements of double-differential cross sections for reactions (n, cp) with respect to the angle and incident energy of the interaction. The Time-of-Flight method is used for the energy determination of the primary neutron and remotely controlled rotating table is used for angle differentiation. The central sample holder can be loaded with up to four different targets which can be switched during the on-beam measurement remotely.

Using the CLID, the neutron flux and energy spectrum were measured by the Proton-Recoil-Telescope (PRT) method. The polyethylene foil (PE,$CH_2$ - 250 µm thick and 2 cm diameter) mounted on the strip of 2.5 µm thin Mylar foil was placed at the center of the chamber and irradiated. The elastically scattered protons were recorded using the telescopes. A carbon sample of the same diameter and half of the thickness was measured in the same position in order

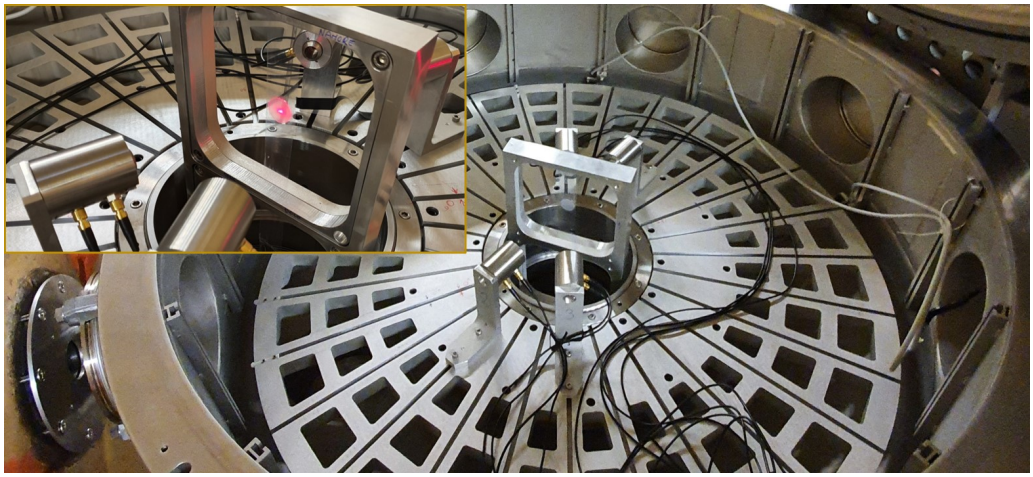

FIGURE 2. The photography of the internal set-up of the CLID placed behind the collimator.

to subtract the background proton events from (n,Xp) reactions on carbon in PE. At last, an yttrium sample was irradiated and analyzed using the activation technique.

The four Si-based telescopes were placed on the rotating table around the irradiated sample, see the Figure 2. Each telescope consisted of two planar Si detectors, the thin one to record the energy loss ($dE$) of the passing charged particle and the thick one to absorb the rest of the particle energy ($E$). In the case of the PRT measurement with the PE foil, the telescope consisted of the 150 µm and 5 mm thick detectors. The solid angle between the PE sample and the telescope was restricted by the circularly shaped aperture with the inner diameter of 8 mm. This solid angle was calculated by numerical integration technique based on the method presented by S. Pommé [15] and the resulting absolute value of 0.00255 sr was obtained. The telescope was placed at the laboratory angle of 45° with respect to the neutron beam axis.

The data acquisition chain consisted of the CAEN preamplifiers and V1730 digitizer. The power supply modules delivering the high- and low-voltage were manufactured by CAEN as well.

## 3. PRT measurement of the neutron spectrum

During the approximately 2-hour-long irradiation of the $CH_2$ target at the beam current of approx. 20 µA the light charged particles were recorded by the PRT at the laboratory angle of 45° and proton events were discriminated by the dE-E method which is graphically represented by the 2-D plot in Figure 3. The energy calibration of the Si-detectors has been performed using the radionuclide $\alpha$-sources with kinetic energies of $\alpha$-particles up to 8 MeV.

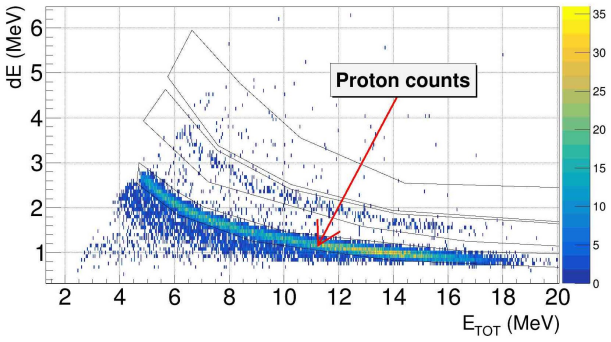


Figure 3. Particle type separation for PRT data.

The background runs were measured with the carbon and empty-holder targets. The background and $^{nat}$C(n,p) proton events were correctly subtracted and the proton spectrum from H(n,p) elastic scattering was reconstructed, see the blue data-set in Figure 4.

To obtain the energy spectrum of protons produced in the PE sample, the unfolding procedure (based on RooUnfold package [16]) was implemented to correct the measured spectra for energy spreading and shifting

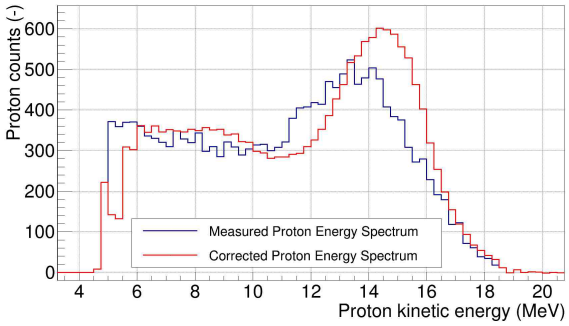


Figure 4. Proton energy spectra measured by PRT (blue) and corrected proton energy spectra (red).

due to the energy loss in the PE sample and due to the variations of the recoil angle within the solid angle of the detector. The response function used for the unfolding process was generated using the Monte-Carlo code Geant4 [17] and the previously created CLID model [18]. The simulated response matrix is plotted in Figure 5 and represents the response of the PRT set-up of the CLID to the theoretical irradiation by the mono-energetic neutrons which are elastically scattered on hydrogen nuclei in PE foil.

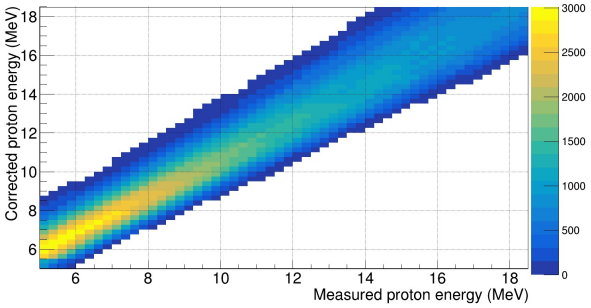


Figure 5. Geant4 simulated response function for the set-up with $CH_2$ target and PRT.

The kinetic energy of protons is recalculated into the energy of interacting neutrons based on the well-defined kinematics of elastic scattering. The following equation is used to calculate the single neutron spectral point in each energy bin of the final neutron spectrum:

$$N_N = \frac{N_P}{\Omega_{lab}\sigma_{diff}H_a b_w C}\,[\mathrm{n/cm^2/MeV/C}], \qquad (1)$$

- $N_P$ – Number of protons detected in the energy bin,
- $\Omega_{lab}$ – Solid angle (in LAB system) from $CH_2$ target to telescope,
- $\sigma_{diff} = \frac{\partial\sigma}{\partial\Omega_{LAB}\partial E_n}$ – ENDF/B-VI Double differential cross-section for H(n,p),
- $H_a$ – number of hydrogen atoms in the $CH_2$ sample,
- $b_w$ – the width of energy bin for which the spectral point is calculated,
- $C$ – the charge of primary proton beam integrated over the period of measurement.

## 4. Activation measurement

Two 12-hours-long irradiations of the yttrium foil were performed. Yttrium is commonly used as activation detector material and has a well-known (n,xn) reaction cross sections. The parameters for two relevant neutron-induced reactions are listed in Table 1. The reaction rates for the production of the $^{88}$Y isotope were successfully measured (with HPGe), while the production of $^{89}$Y(n,3n)$^{87}$Y could not be measured due to the long cooling times of the yttrium foil compared to the relatively short half-life period.

| **Reaction** | **Q-value** [MeV] | **Threshold** [MeV] | **Half life** [days] |
|---|---|---|---|
| $^{89}$Y(n,2n)$^{88}$Y | -11.48 | 11.61 | 106.65 |
| $^{89}$Y(n,3n)$^{87}$Y | -20.83 | 21.07 | 3.33 |

Table 1. Basic reaction parameters relevant for activation technique assessment.

The overview of experimental and evaluated cross-section data for the $^{89}$Y(n,2n)$^{88}$Y reaction plotted by JANIS [19] is shown In Figure 6. The measured

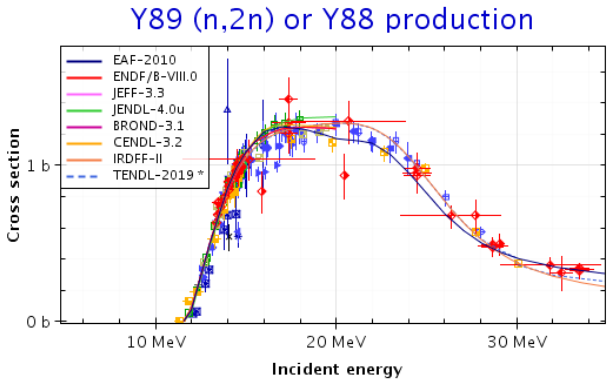


Figure 6. Experimental and evaluated cross-section data for $^{89}$Y(n,2n)$^{88}$Y reaction plotted by JANIS [19].

reaction rates can be used to control the correctness of the absolute values in the neutron spectra measured by the PRT technique as will be shown in the following Section 5.

## 5. Results

The neutron energy spectrum at the irradiation position of the CLID was measured by the PRT technique and calculated using the Eq. 1 together with the measured proton data presented in Figure 4. The resulting neutron energy spectrum is plotted in Figure 7.

The reaction rates (number of produced nuclei per 1 g of the sample and per 1 primary particle) for the production of $^{88}$Y isotope were measured by the HPGe detectors. Besides the activation technique described in the previous Section 4, the reaction rate was also calculated by the integration of the known cross-section $\sigma(E)$ (Figure 6) with the PRT-measured

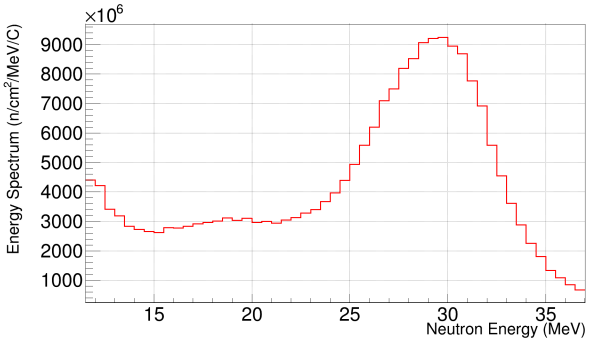


Figure 7. Spectral neutron flux measured by the PRT method with the CLID.

neutron flux $\phi(E)$ over the energy range of the neutron energy spectrum in Figure 7:

$$R_R = \int_{E_{min}}^{E_{max}} \sigma(E)\phi(E)dE, \qquad (2)$$

where $E$ is the neutron kinetic energy. The neutron cross-section data for $\sigma(E)$ were taken from the EAF-2010 [20] data library. The absolute values for the $R_R$ quantity calculated by both approaches (activation method, PRT method) are listed in the Table 2. The resulting normalization factor is listed as well and the disagreement between the two measured values is further explained in the conclusion of this article.

| **$R_R$ by Activation method** [/g/C] | **$R_R$ for PRT method** [/g/C] | **Normalization factor** [-] |
|---|---|---|
| 6.71E+08 | 4.85E+08 | 1.3844 |

Table 2. The reaction rates calculated for $^{89}$Y(n,2n)$^{88}$Y reaction and their ratio.

In the Figure 8 the final neutron energy spectrum measured by the PRT technique and corrected by the normalization factor deduced from activation measurement with yttrium sample is shown.

An independent measurement with the NE213 scintillator in the ToF mode was performed to obtain the neutron spectral flux at the irradiation position of the CLID. The methodology of the TOF measurement is beyond the scope of this paper [21, 22]. The resulting ToF neutron spectrum is shown in Figure 8 for comparison.

Furthermore, the MCNPX [23] calculation was performed to simulate the neutron flux in the CLID irradiation position. The complete geometry with the collimator was used in the MCNPX simulation, the beryllium target backed with the carbon slab and the layer of coolant in the target station was modelled. The neutron production was simulated for the p(34.8 MeV)+$^{9}$Be(2.5 mm thick) reaction using the JENDL4.0/HE data library [24, 25]. Comparison between experimentally measured neutron fluxes and MCNPX simulation is shown in Figure 8 as well.

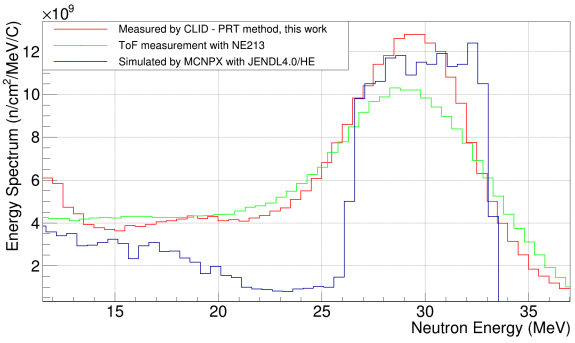


Figure 8. Spectral neutron fluxes measured by PRT method and normalized by $^{88}$Y production rates (red), measured by the NE213 (green) and simulated by the MCNPX code using the JENDL4.0/HE data library (blue)[24, 25].

For all three energy spectra plotted in Figure 8, the absolute values of the QM-peak neutrons measured or simulated at the CLID irradiation position were integrated, see the Table 3. The lower integration limits were 20 MeV, 21 MeV and 23 MeV for data sets from NE213, PRT and MCNPX respectively. Both measurements (NE213, normalized PRT) are in very good agreement with each other. On the other hand, the MCNPX simulation gives roughly 30 % lower values for the QM-peak integral compared to the measurements. This disagreement with the MCNPX results is probably due to the poor precision of the implemented cross-section data for the production of neutrons in the JENDL4.0/HE library. The JENDL4.0/HE has however better description of the neutron production than the other existing library ENDF7PROT [26] and therefore was chosen for this comparison.

| | **NE213 ToF** | **PRT normalised** | **MCNPX simulation** |
|---|---|---|---|
| Peak neut. [n/cm$^2$/C] | 1.10E+11 | 1.11E+11 | 8.067E+10 |

Table 3. Integral values of QM neutrons at the CLID irradiation position.

## 6. Conclusions

This paper describes the overall experimental set-up with the new vacuum chamber. The implementation of the PRT technique for neutron flux determination with the CLID was described in detail. During the one weekend-long on-beam experiment with the CLID, the $CH_2$, $^{89}$Y and $^{nat}$C targets were irradiated and the measured data were used for the characterization of the fast neutron spectrum in the collimated beam.

The detailed analysis of the experimental data has shown that some events were randomly lost during the data acquisition or their energy deposition values were falsely recorded. The evidence for this effect can be found around the proton band in Figure 3. This issue was already addressed and solved for future experiments. The experimental PRT data presented in this paper were however compromised and consequently had to be normalised. The normalisation factor was deduced from the activation measurement of the irradiated yttrium sample. The $^{89}$Y(n,2n)$^{88}$Y reaction has very well known cross section (Figure 6) in the energy range from 11 MeV to 36 MeV. The correctness of the activation measurement was confirmed by the ToF measurements performed with the organic scintillator NE213. The $R_R = 6.711E08$ $^{88}$Y/g/C value calculated for the neutron energy spectrum (green in Figure 8) measured by the NE213 matches perfectly with the $R_R$ value presented for activation in Table 2. The ToF spectrum agrees with the normalized PRT neutron energy spectrum.

The integral values for QM-peak neutron fluxes (as presented in Table 3) are of the key importance for every experiment on collimated fast neutron beams produced on 2.5 mm thin beryllium target by the cyclotron U-120M at energies around 34.8 MeV. The overall relative uncertainty of the measured data in Table 3 is expected to be below 10 %. The accuracy of the MCNPX/JENDL4.0/HE predicted values is lower because of the worse implementation of the neutron production in the JENDL4.0/HE evaluation. The broad QM peak from the p+Be reaction on 2.5 mm thin beryllium target is composed of two narrow peaks which originate from the ground and excited states of the remaining $^9B$ nucleus [14]. The absolute values of cross section and the intensity ratio between these two inner peaks is not implemented correctly into the evaluated data libraries. The production of neutrons is however better described in JENDL4.0/HE than in the other existing libraries generally used with MCNPX.

## Acknowledgements

This project has received funding from the European Union's Horizon 2020 research and innovation programme under grant agreement No 847552.

This work was supported by OP RDE, MEYS, CZ under the project CANAM, EF16_013/0001812.

Computational resources were supplied by the project "e-Infrastruktura CZ" (e-INFRA CZ LM2018140) supported by the Ministry of Education, Youth and Sports of the Czech Republic.

This work was supported by the Grant Agency of the Czech Technical University in Prague, grant No. SGS18/145/OHK4/2T/14.

## References

[1] P. Lisowski, C. Bowman, G. Russell, S. Wender. The Los Alamos National Laboratory Spallation Neutron Sources. *Nuclear Science and Engineering* **106**(2):208–218, 1990. https://doi.org/10.13182/NSE90-A27471.

[2] C. Dufauquez, I. Slypen, S. Benck, et al. Light Charged Particle Production in Fast Neutron-induced Reactions on Carbon (En=40 to 75 MeV): (II). Tritons and Alpha Particles. *Nuclear Physics A* **671**(1):20–32, 2000. https://doi.org/10.1016/S0375-9474(99)00827-1.

[3] S. Benck, I. Slypen, V. Corcalciuc, J. Meulders. Neutron-proton Differential Cross Section Measurements for En from 28 to 75 MeV. *Nuclear Physics A* **615**(2):220–228, 1997. https://doi.org/10.1016/S0375-9474(96)00484-8.

[4] I. Slypen, S. Benck, J. Meulders, V. Corcalciuc. Light Charged Particle Production in Fast Neutron-induced Reactions on Carbon (En=20 to 75 MeV): (I). Protons and Deuterons. *Nuclear Physics A* **671**(1):3–19, 2000. https://doi.org/10.1016/S0375-9474(99)00829-5.

[5] F. Brady, C. Castaneda, G. Needham, et al. Isovector and Gamow-teller Strength from Small-angle $(n, p)$ Reactions at 60 MeV. *Physical Review Letters* **48**:860–863, 1982. https://doi.org/10.1103/PhysRevLett.48.860.

[6] F. Brady, G. Needham, J. Romero, et al. New Giant Dipole Strength in $^{6}$Li and $^{7}$Li as Revealed via $(n, p)$ at 60 MeV. *Physical Review Letters* **51**:1320–1323, 1983. https://doi.org/10.1103/PhysRevLett.51.1320.

[7] T. Subramanian, J. Romero, F. Brady, et al. Double Differential Inclusive Hydrogen and Helium Spectra from Neutron-induced Reactions on Carbon at 27.4, 39.7, and 60.7 MeV. *Physical Review C* **28**:521–528, 1983. https://doi.org/10.1103/PhysRevC.28.521.

[8] S. Pomp, R. Bevilacqua, M. Hayashi, et al. A Medley with over Ten Years of (Mostly) Light-ion Production Measurements at The Svedberg Laboratory. *EPJ Web of Conferences* **8**:07013, 2010. https://doi.org/10.1051/epjconf/20100807013.

[9] U. Tippawan, T. Vilaithong, S. Pomp, et al. Light-ion Production in 175 MeV Neutron-induced Reactions on Oxygen. *Nuclear Data Sheets* **119**:194–196, 2014. https://doi.org/10.1016/j.nds.2014.08.054.

[10] V. Blideanu, F. Lecolley, J. Lecolley, et al. Nucleon-induced Reactions at Intermediate Energies: New Data at 96 MeV and Theoretical Status. *Physical Review C* **70**:014607, 2004. https://doi.org/10.1103/PhysRevC.70.014607.

[11] U. Tippawan, S. Pomp, J. Blomgren, et al. Double-differential Cross Sections and Kerma Coefficients for Light-charged Particles Produced by 96 MeV Neutrons on Carbon. *Radiation Measurements* **45**(10):1134–1138, 2010. https://doi.org/10.1016/j.radmeas.2010.06.030.

[12] C. Gustavsson, S. Pomp, G. Scian, et al. Nuclear Data Measurements at the New NFS Facility at GANIL. *Physica Scripta* **2012**(T150):014017, 2012. https://doi.org/10.1088/0031-8949/2012/t150/014017.

[13] L. Liu, K. Sun, H. Yi, et al. Measurement of Differential Cross Sections of Neutron-induced Alpha Production Reactions on Carbon from 6.3 to 102.3 MeV, 2022. https://doi.org/10.48550/ARXIV.2209.02963.

[14] J. Novák, P. Bém, M. Majerle, et al. The p(thin target) Reaction as a Source of Quasi-monoenergetic Neutrons. *EPJ Web of Conferences* **146**:03013, 2017. https://doi.org/10.1051/epjconf/201714603013.

[15] S. Pommé, L. Johansson, G. Sibbens, B. Denecke. An Algorithm for the Solid Angle Calculation Applied in Alpha-particle Counting. *Nuclear Instruments and Methods in Physics Research Section A: Accelerators, Spectrometers, Detectors and Associated Equipment* **505**(1):286–289, 2003. Proceedings of the tenth Symposium on Radiation Measurements and Applications, https://doi.org/10.1016/S0168-9002(03)01070-2.

[16] T. Adye. Unfolding Algorithms and Tests Using RooUnfold, 2011. http://arxiv.org/abs/1105.1160.

[17] S. Agostinelli, J. Allison, K. Amako, et al. Geant4—a Simulation Toolkit. *Nuclear Instruments and Methods in Physics Research Section A: Accelerators, Spectrometers, Detectors and Associated Equipment* **506**(3):250–303, 2003. https://doi.org/10.1016/S0168-9002(03)01368-8.

[18] M. Ansorge. Geant4 model reakční vakuové komory CLID Česká nukleární společnost z.s., 2020. ISBN 978-80-02-02895-6.

[19] N. Soppera, M. Bossant, E. Dupont. JANIS 4: An Improved Version of the NEA Java-based Nuclear Data Information System. *Nuclear Data Sheets* **120**:294–296, 2014. https://doi.org/10.1016/j.nds.2014.07.071.

[20] J. Sublet, et al. The European Activation File: EAF-2010 Neutron-induced Cross Section Library 2010.

[21] J. Novák, M. Ansorge, P. Bém, et al. New Detection Systems at U-120M Cyclotron. *EPJ Web of Conferences* **239**:17020, 2020. https://doi.org/10.1051/epjconf/202023917020.

[22] M. Ansorge, P. Bém, D. Hladík, et al. Total Neutron Cross-section Extracted from Transmission Experiments with Liquid Oxygen Using Neutron Energies from 18 to 27 MeV. *EPJ Web of Conferences* **239**:20008, 2020. https://doi.org/10.1051/epjconf/202023920008.

[23] D. Pelowitz. MCNPX Users Manual Version 2.7.0. *LA-CP-11-00438* 2011.

[24] K. Shibata, O. Iwamoto, T. Nakagawa, et al. JENDL-4.0: A New Library for Nuclear Science and Engineering. *Jurnal of Nuclear Science and Technology* **48**(1):1–30, 2011. https://doi.org/10.1080/18811248.2011.9711675.

[25] S. Kunieda, et al. Overview of JENDL-4.0/HE and Benchmark Calculation. *JAEA-Conf* **004**:41–46, 2016. https://doi.org/10.11484/jaea-conf-2016-004.

[26] H. Trellue, R. Little, White, et al. New ACE-Formatted Neutron and Proton Libraries Based on ENDF/B-VII.0. *Nuclear technology* 2008.